Localization and percolation in semiconductor alloys: GaAsN vs GaAsP

L. Bellaiche, S.-H. Wei, and Alex Zunger
National Renewable Energy Laboratory, Golden, Colorado 80401
(Received 29 July 1996)

Tradition has it that in the absence of structural phase transition, or direct-to-indirect band-gap crossover, the properties of semiconductor alloys (bond lengths, band gaps, elastic constants, etc.) have simple and smooth (often parabolic) dependence on composition. We illustrate two types of violations of this almost universally expected behavior. First, at the percolation composition threshold where a continuous, wall-to-wall chain of given bonds (e.g., Ga-N-Ga-N⋯) first forms in the alloy (e.g., $GaAs_{1-x}N_x$), we find an anomalous behavior in the corresponding bond length (e.g., Ga-N). Second, we show that if the dilute alloy (e.g., $GaAs_{1-x}N_x$ for $x\rightarrow 1$) shows a localized deep impurity level in the gap, then there will be a composition domain in the concentrated alloy where its electronic properties (e.g., optical bowing coefficient) become irregular: unusually large and composition dependent. We contrast $GaAs_{1-x}N_x$ with the weakly perturbed alloy system $GaAs_{1-x}P_x$ having no deep gap levels in the impurity limits, and find that the concentrated $GaAs_{1-x}P_x$ alloy behaves normally in this case. [S0163-1829(96)10648-2]

I. INTRODUCTION

In the absence of composition-induced structural phase transitions in alloys [e.g., zinc-blende-to-wurtzite in CdTeSe (Ref. 1) and zinc-blende-to-NiAs in MnCdTe (Ref. 2)] or electronic direct-to-indirect band gap crossovers [e.g., AlGaAs (Refs. 3 and 4) and AlGaAsP (Refs. 5–8)], physical properties $P(x)$ were traditionally assumed[9] to be simple continuous functions of the composition x. This strongly held view is reflected by the almost universal depiction of the composition dependence of $P(x)$ by simple analytic form,[9] e.g., a linear (Vegard-like) term, plus a small quadratic correction:

$$P(x)=[xP(A)+(1-x)P(B)]-bx(1-x), \qquad (1)$$

where $P(A)$ and $P(B)$ are the properties of the constituents A and B of the alloy A_xB_{1-x}, and b is the ''bowing coefficient.'' Examples[9] of Eq. (1) include P=lattice parameters, band gaps (b is then called ''optical bowing coefficient''), and mixing enthalpy (b is then called ''interaction parameter''). In all cases, b is composition independent. The optical bowing coefficient of conventional semiconductor alloys is known[9] to be small (lower than 1 eV).

Exceptions to this analytic and regular behavior are known to occur in some *metallic alloys*, when changes in composition move the Fermi level through a Van-Hove singularity (i.e., ''electronic topological transitions''[10,11]), and in some *semiconductor alloys* (e.g., PbCdTe, PbSnTe, and PbGeTe) (Ref. 12) showing some irregularities in microhardness, Hall mobility, and charge-carrier concentration at very dilute alloys. Because of the tediousness of measuring alloy properties on a sufficiently dense mesh of compositions, and because of the prevailing paradigm of the continuity and smoothness of $P(x)$, irregularities in $P(x)$ might have been previously overlooked or ''smoothed over.'' Likewise, theoretical calculations of alloy properties are often based on small supercells,[13–15] restricting explorations to only sparsely spaced discrete compositions. Possible irregular behavior of $P(x)$ in a narrow composition range could have been easily overlooked.

In the present study, we address the general question of the possibility of irregular behavior of $P(x)$ vs x in alloys lacking structural, topological, or electronic direct-to-indirect transitions. Our working hypothesis is that if an $A_xB_{1-x}C$ semiconductor alloy exhibits in the dilute impurity limit $x\rightarrow 0$ or $x\rightarrow 1$ a bound impurity gap state, there could be a composition domain around these compositions where the alloy properties will be irregular [i.e., violate Eq. (1) for which b is a constant]. We know from the work of Slater and Koster[16] that a bound impurity state exists when the impurity and host atoms have sufficiently different properties. We have thus selected an alloy system $GaAs_{1-x}N_x$ whose bulk components (although isovalent, isostructural, and insulating) do manifest significant relative differences in physical properties: zinc-blende GaAs and GaN have a large size difference ($\Delta a/a>20\%$), the Ga-N bond is more than twice as stiff as the Ga-As bond, and there is a large difference in atomic valence s and p orbital energies between As and N ($\simeq$4 and $\simeq$2 eV for s and p, respectively). Because of the large magnitude of the mutual perturbations of the alloyed elements, if irregularities exist in $P(x)$, their amplitude would be noticeable. As a counterexample we selected $GaAs_{1-x}P_x$ whose bulk components show little difference.

We find that there is a significant *structural* anomaly at those compositions where a continuous chain of bonds forms in an alloy medium, e.g., Ga-N-Ga-N⋯ or Ga-As-Ga-As⋯ in the $GaAs_{1-x}N_x$ alloy. This occurs at the impurity percolation threshold $x_p=0.19$ for the fcc lattice. In addition (and independently), we find that whenever the impurity limit exhibits deep impurity gap levels, there are *electronic* anomalies in the corresponding alloy, manifested by a composition dependence of the bowing coefficient b of Eq. (1). This study thus points to two interesting cases—percolation and impuritylike localization—where the physical picture underlying Eq. (1) is invalid.

 © 1996 The American Physical Society

TABLE I. Structural relaxations parameters u_{Ga} (dimensionless and equal to 0.25 in the unrelaxed structure) of some ordered $GaAs_{1-x}N_x$ alloys as calculated by the LAPW method and by the VFF method. We also give the optical bowing coefficients b [Eq. (1)] obtained by LAPW and by the empirical pseudopotentials method, using either the LAPW structural parameters (EPM1) or the VFF structure parameters (EPM2). The ordered structures are defined in Ref. 20.

	u_{Ga}		b (eV)		
Structure	LAPW	VFF	LAPW	EPM1	EPM2
$D1$ (Ga_8As_7N)	0.220	0.216	15.7	10.7	12.1
$L1_2$ (Ga_4As_3N)	0.223	0.217	6.7	7.9	9.8
CuPt (Ga_2AsN)	0.222	0.223	11.5	8.4	10.4
$L1_2$ (Ga_4AsN_3)	0.274	0.278	11.7	14.8	18.0
$D1$ (Ga_8AsN_7)	0.276	0.278	15.8	20.4	22.4

II. METHOD OF CALCULATION

We use a large (512-atom) supercell representation of $GaAs_{1-x}N_x$ and $GaAs_{1-x}P_x$ alloys, ''flipping'' one-by-one As into N or P, thus allowing small steps ($\Delta x = 0.004$) in composition and a fixed supercell symmetry for all compositions. For each composition, we distribute the mixed elements at random on the fcc anion lattice sites, fully relaxing atomic positions via a conjugate gradient minimization of a parametrized valence force field (virtually all atoms end up being displaced away from the ideal zinc-blende sites). The lattice constant of the alloys is assumed here to vary linearly as a function of the composition x so as not to introduce any bias at some composition range. A near-Vegard behavior was actually found for $GaAs_{1-x}N_x$ in first-principles local-density approximation (LDA) total energy calculations.[14,15] The relaxed atomic positions in each supercell configuration are obtained by minimizing the valence force field (VFF) energy.[17,18] We used the bond-stretching (α) and bond-bending (β) force constants of Ref. 19 for GaN (α=96.30 N/m and β=14.80 N/m) and of Ref. 18 for GaAs (α=41.19 N/m and β=8.94 N/m) and for GaP (α=47.32 N/m and β=10.44 N/m). To test the adequacy of VFF, Table I compares the calculated structural relaxation parameters of some *ordered* $GaAs_{1-x}N_x$ alloys[20] using the VFF and using the first-principles linearized augmented plane wave (LAPW) method.[14] We find that the VFF follows the structural trends in the first-principles results reasonably well.

The electronic properties of the relaxed supercell are obtained via a plane-wave pseudopotential approach, using local empirical pseudopotentials that are carefully fitted to physical properties of the bulk constituents. The crystal potential $V(\mathbf{r})$ of the alloys is written as a superposition of atomic pseudopotentials $v_\alpha(\mathbf{r})$ (α=Ga,N,P,As), and the Fourier transform of $v_\alpha(\mathbf{r})$ is represented as

$$v_\alpha(q) = \Omega_\alpha \sum_{l=1}^{4} [a_{l\alpha} e^{-b_{l\alpha}(q-c_{l\alpha})^2}], \qquad (2)$$

where Ω_α is an atomic normalization volume. Using the gallium pseudopotentials of Ref. 21, the nitrogen and phosphorus parameters of Eq. (2) were fitted carefully to the many-body-corrected (GW) band structures,[22,23] experimental band gaps,[24,25] and LDA deformation potentials. We use the As pseudopotential of Ref. 21. Tables II, III, and IV summarize the results for GaN, GaP, and GaAs, respectively. The parameters of Eq. (2) for Ga, N, P, and As are given in Table V. Due to the large lattice mismatch between GaAs and GaN, we have fitted the pseudopotentials using a composition-dependent kinetic energy cutoff in order to keep the same number of plane waves per zinc-blende cell for all the compositions (i.e., volumes). This kinetic energy cutoff is 5 Ry for GaAs and GaP, and 7.87 Ry for GaN, corresponding, in all cases, to 59 plane waves at Γ per zinc-blende cell. Our pseudopotentials must be used at this (fixed) number of plane waves. These empirical potentials are designed and fitted so as to be used with a rather small kinetic energy cutoff, in order to be able to treat large systems with a satisfactory accuracy.[21] Table I compares the calculated optical bowing coefficients for some ordered $GaAs_{1-x}N_x$ alloys obtained by the LAPW method and by our empirical pseudopotential method. The agreement in the trends seen in the two methods is good.

TABLE II. Comparison of the electronic energy levels and the hydrostatic deformation potentials dE/dP of the zinc-blende GaN calculated by the present empirical pseudopotentials (EPM) and by various *ab initio* calculations. The zero of energy levels is chosen at the top of the valence band. The natural band offset between zinc-blende GaAs and GaN is fitted to 2.28 eV (the LAPW value of the present work). The effective mass $m(\Gamma_{1c})$ at the conduction-band minimum is also given. The plane-wave energy cutoff is 7.87 Ry at the equilibrium lattice constant of 4.51 Å. The experimental direct band gap is 3.27 eV (Ref. 24).

Zinc-blende GaN	EPM	GW1[a]	GW2[b]	LDA[c]
Energy levels (eV):				
Γ_{1c} (gap)	3.27	3.1	2.8	1.73
Γ_{15c}	10.55	12.2	11.3	10.08
X_{3v}	−6.06	−6.9	−6.8	−6.23
X_{5v}	−2.58	−3.0	−2.9	−2.74
X_{1c}	4.59	4.7	4.0	3.27
X_{3c}	7.30	8.4	7.7	6.47
$L_{1v}^{(2)}$	−6.55	−7.8	−7.5	−7.13
$L_{1v}^{(3)}$	−0.86	−1.1	−1.0	−0.99
$L_{1c}^{(1)}$	5.88	6.2	5.7	4.52
$L_{1c}^{(2)}$	10.42	11.2	10.4	8.61
dE/dP (meV/kbar):				
$\Gamma_{15v}-\Gamma_{1c}$	3.49			3.53
$\Gamma_{15v}-X_{1c}$	−0.21			0.21
$\Gamma_{15v}-L_{1c}^{(1)}$	2.39			3.72
$m(\Gamma_{1c})$	0.129			

[a]Reference 22 (a=4.50 Å).
[b]Reference 23 (a=4.50 Å).
[c]LAPW, present work (a=4.51 Å).

Having established the reliability of our computational scheme for the binary constituents (Tables II–IV) and for small unit cell ordered compounds (Table I), we next turn to the large supercell random alloy. To calculate near-gap energy levels of large supercells, we use the ''folded spectrum method'':[37] this is an ''O(N) method,'' producing exact

TABLE III. Comparison of the electronic energy levels and the hydrostatic deformation potentials dE/dP of the zinc-blende GaP obtained by the present empirical pseudopotentials (EPM), experiment, and by *ab initio* calculations. The zero of energy levels is chosen at the top of the valence band. The natural band offset between zinc-blende GaAs and GaP was fit to 0.33 eV (the LDA value of Ref. 26). The effective mass $m(\Gamma_{1c})$ at Γ_{1c} is also given. The plane-wave energy cutoff is 5 Ry at the equilibrium lattice constant of 5.45 Å.

Zinc-blende GaP	EPM	Experiment[a]	LDA[b]
Γ_{15v}(GaP)-Γ_{15v}(GaAs) (eV)	−0.31		−0.33
Energy levels (eV):			
Γ_{1c}	2.86	2.86	1.52
Γ_{15c}	4.61		3.72
X_{3v}	−6.21	−6.40	−6.95
X_{5v}	−2.39	−2.90	−2.78
X_{1c} (gap)	2.33	2.32	1.50
X_{3c}	2.72		1.67
$L_{1v}^{(2)}$	−6.10		6.80
$L_{1v}^{(3)}$	−0.97		−1.18
$L_{1c}^{(1)}$	2.65	2.67	1.44
$L_{1c}^{(2)}$	5.39		4.65
dE/dP (meV/kbar):			
$\Gamma_{15v}-\Gamma_{1c}$	9.2		9.0
$\Gamma_{15v}-X_{1c}$	−1.6		−2.0
$\Gamma_{15v}-L_{1c}^{(1)}$	3.5		3.3
$m(\Gamma_{1c})$	0.130		

[a]Reference 25.
[b]LAPW, present work ($a=5.45$ Å).

TABLE IV. Comparison of the electronic energy levels, the hydrostatic deformation potentials dE/dP, and the effective mass $m(\Gamma_{1c})$ at Γ_{1c} of the zinc-blende GaAs obtained by the empirical pseudopotentials (EPM), experiment, and by *ab initio* calculations. The zero of energy levels is chosen at the top of the valence band. The plane-wave energy cutoff is 5 Ry at the equilibrium lattice constant of 5.65 Å.

Zinc-blende GaAs	EPM	Experiment	GW[b]	LDA[f]
Energy levels (eV):				
Γ_{1c} (gap)	1.52	1.52[a]	1.47	
Γ_{15c}	4.01	4.72[c]	4.52	
X_{3v}	−6.24			
X_{5v}	−2.33	−2.80[c]	−2.73	
X_{1c}	2.00	1.98[d]	2.08	
X_{3c}	2.32	2.38[d]	2.30	
$L_{1v}^{(2)}$	−5.95			
$L_{1v}^{(3)}$	−0.96	−1.30[c]	−1.11	
$L_{1c}^{(1)}$	1.81	1.81[d]	1.82	
$L_{1c}^{(2)}$	4.85			
dE/dP (meV/kbar):				
$\Gamma_{15v}-\Gamma_{1c}$	8.46	10.82[e]		10.3
$\Gamma_{15v}-X_{1c}$	−2.51	−1.26,[g] −1.8[h]		−2.2
$\Gamma_{15v}-L_{1c}^{(1)}$	2.59	5.5[i]		3.9
$m(\Gamma_{1c})$	0.077	0.066[j]		

[a]Reference 27.
[b]Reference 28.
[c]Reference 29.
[d]Reference 30.
[e]Reference 31.
[f]Reference 32.
[g]Reference 33.
[h]Reference 34.
[i]Reference 35.
[j]Reference 36.

eigensolutions in a given energy window. At each composition, results are averaged over a few, randomly selected configurations. The resulting wave functions are analyzed by defining a localization parameter $Q_{\alpha,i}$ (α=Ga, As, or N, and i=VBM or CBM) as

$$Q_{\alpha,i}=\frac{F}{N_\sigma N_\alpha}\frac{1}{[a(x)]^3}\sum_\sigma \sum_{j\in\alpha}\int_{V_j}|\psi_i^\sigma|^2 dV, \qquad (3)$$

where the sums are over the N_σ random configurations (four in the present study) at composition x and over all the atomic sites j of type α. Here F is an arbitrary factor (equal to 27), N_α is the number of atoms of type α, $a(x)$ is the lattice constant of the alloy, and the integration of the square of the wave function ψ_i^σ is performed in a volume $V_j=\{[a(x)/6]\}^3$ centered around atoms j of type α.

III. RESULTS

A. Dilute alloys: The impurity limit

To demonstrate the qualitative difference between $GaAs_{1-x}N_x$ and $GaAs_{1-x}P_x$, we contrast in Tables VI and VII the properties of the dilute alloys. Table VI describes first the properties of the *dilute* $GaAs_{1-x}N_x$ alloy (one impurity in a 512-atom cell), for $x\rightarrow 0$ (N impurity in GaAs) and $x\rightarrow 1$ (As impurity in GaN). We see that (i) Ga<u>As</u>:N is characterized by a resonant level in the conduction band[38,39] and a N-perturbed CBM, but no gap level. On the other hand, (ii) Ga<u>N</u>:As is characterized by a *deep*, nearly composition-independent impurity level at $\epsilon_{\mathrm{VBM}}+0.75$ eV (close to the experimental estimate[40] of 0.87 eV for the wurtzite structure). Its wave function is strongly localized on the arsenic impurity ($Q=178$, compared to 4.2 in the pure GaN host). There is only a partial relaxation of the nearest-neighbor bonds ($R_{\text{Ga-As}}$=2.25 Å compared to 2.45 Å in GaAs). Clearly, a large and less electronegative impurity in a small host (Ga<u>N</u>:As) poses a more severe perturbation (for gap levels) than a small and more electronegative impurity in a large host (Ga<u>As</u>:N).

To check our conjecture that the alloy properties of systems with localized impurity levels are different than those without such levels, we have examined a paradigm ‘‘weakly interacting’’ alloy system: $GaAs_{1-x}P_x$. The mismatch in bond stiffness (13%), lattice constants (3.6%), and orbital energies (0.7 and 0.3 eV for s and p orbitals) between the two endpoints is rather small. The dilute alloy limit of Ga<u>As</u>:P and Ga<u>P</u>:As have no gap levels.

TABLE V. Atomic pseudopotential parameters used in this study. The four rows for each atom correspond to the four Gaussians in Eq. (2). These pseudopotentials must be used with a constant number of plane waves of 59 per zinc-blende cell, corresponding to the kinetic energy cutoff of 5 Ry for GaAs and GaP and of 7.87 Ry for GaN.

Atom	$\alpha\ \Omega_\alpha$ (a.u.)^3	l	$a_{l\alpha}$ (Ry)	$b_{l\alpha}$ (a.u.)$^{-1}$	$c_{l\alpha}$ (a.u.)^2
Ga	131.4				
		1	−1.244 980 0	1.527 480	0.0
		2	0.046 435 7	0.574 047	2.019 35
		3	0.036 651 7	0.959 082	2.097 82
		4	−0.013 338 5	11.270 800	2.935 81
As	145.2				
		1	−1.058 210 0	0.959 327	0.0
		2	−0.043 431 2	2.946 790	0.851 64
		3	0.105 690 0	0.820 922	1.224 36
		4	−0.002 176 3	6.531 450	2.468 08
N	75.0				
		1	−0.226 280 0	1.816 013	0.0
		2	−0.926 830 0	0.918 842	0.851 77
		3	0.237 280 0	0.909 593	1.555 91
		4	0.020 830 0	13.519 21	2.628 52
P	139.2				
		1	−1.028 210 0	0.870 327	0.0
		2	−0.049 431 0	3.186 790	0.889 64
		3	0.117 690 0	0.470 922	1.028 36
		4	0.012 176 0	5.811 450	2.400 80

TABLE VI. Structural and electronic properties of N impurity in GaAs (GaAs:N) and As impurity in GaN (GaN:As). The charges Q are calculated from Eq. (3) using a 512-atom cell. $R_{\text{Ga-N}}$ and $R_{\text{Ga-As}}$ are the nearest-neighbor bond lengths. Note that GaAs:N has no gap level[38] while GaN:As has a deep, localized level.

Property	GaAs and GaAs:N	GaN and GaN:As
Pure host:		
Q_{VBM} (anion)	1.55	4.16
Q_{VBM} (cation)	0.51	0.30
Q_{CBM} (anion)	3.19	4.81
Q_{CBM} (cation)	1.64	1.18
$R_{\text{Ga-As}}$ (Å)	2.45	
$R_{\text{Ga-N}}$ (Å)		1.95
Impurity:		
$Q_{\text{impurity level}}$		1.0 (Ga) 178 (As) 1.9 (N)
$R_{\text{Ga-N}}$ (Å)	2.03	1.95
$R_{\text{Ga-As}}$ (Å)	2.45	2.25
Energy level (eV)		$\epsilon_{\text{VBM}}+0.75$

TABLE VII. Structural and electronic properties of P impurity in GaAs (GaAs:P) and As impurity in GaP (GaP:As). The charges Q are calculated from Eq. (3) using a 512-atom cell. $R_{\text{Ga-P}}$ and $R_{\text{Ga-As}}$ are the nearest-neighbor bond lengths. Note that GaAs:P and GaP have no gap levels.

Property	GaAs and GaAs:P	GaP and GaP:As
Pure host:		
Q_{VBM} (anion)	1.55	1.86
Q_{VBM} (cation)	0.51	0.46
Q_{CBM} (anion)	3.19	0.59
Q_{CBM} (cation)	1.64	0.43
$R_{\text{Ga-As}}$ (Å)	2.45	
$R_{\text{Ga-P}}$ (Å)		2.36
Impurity:		
$Q_{\text{impurity level}}$		
$R_{\text{Ga-P}}$ (Å)	2.38	2.36
$R_{\text{Ga-As}}$ (Å)	2.45	2.42
Energy level (eV)		

B. The full alloy range

1. Alloy bond lengths and the appearance of percolation thresholds

We next raise gradually the composition from the dilute impurity limits to cover the full alloy range. Figure 1 shows the nearest-neighbor distances $R_{\text{Ga-As}}(x)$ and $R_{\text{Ga-N}}(x)$ versus x in $\text{GaAs}_{1-x}\text{N}_x$, demonstrating a bimodal distribution. We are not aware of any experimental determination of these bond lengths in this alloy system. Figure 2 shows similar results for $\text{GaAs}_{1-x}\text{P}_x$, and Table VIII compares our calculated results to the measured extended x-ray absorption fine structure (EXAFS) data of Ref. 41 for this system, showing good agreement. Figure 1(b) shows an enlarged section of $R_{\text{Ga-N}}(x)$ revealing a small slope discontinuity at $x_p\sim0.19$. To test whether this result is accidental or not, we have repeated the VFF calculation with a larger supercell containing 1000 atoms, taking an average of eight configurations at each composition. The calculated Ga-N bond length exhibits again a slight slope discontinuity near x_p. We interpret this anomaly as the appearance of a percolation threshold. In the site percolation model for a regular lattice,[42] a property, which carries the statistical character of the problem, is randomly assigned to each site of the regular lattice, and the percolation threshold is defined as the minimum composition of the assigned sites forming an infinite connected cluster, which thus allows the propagation of the property through the whole sample. In line with this idea, we have analyzed our 512-atom supercell searching for the composition at which a connected chain of N-N bonds first forms on the fcc anion sublattice. We find $x_p=0.19$, close to the more accurate result of $x_p=0.198$ (Ref. 43) obtained in previous fcc percolation simulations. Thus, at $x_p\simeq0.19$, one forms a continuous chain of *stiff* Ga-N-Ga-N$\cdots$ bonds in a soft alloy medium ($\alpha_{\text{VFF}}=96.30$ N/m for GaN, compared to $\alpha_{\text{VFF}}=41.19$ N/m for GaAs). Interestingly, the formation of a continuous chain of *soft* Ga-As-Ga-As bonds in a stiffer al-

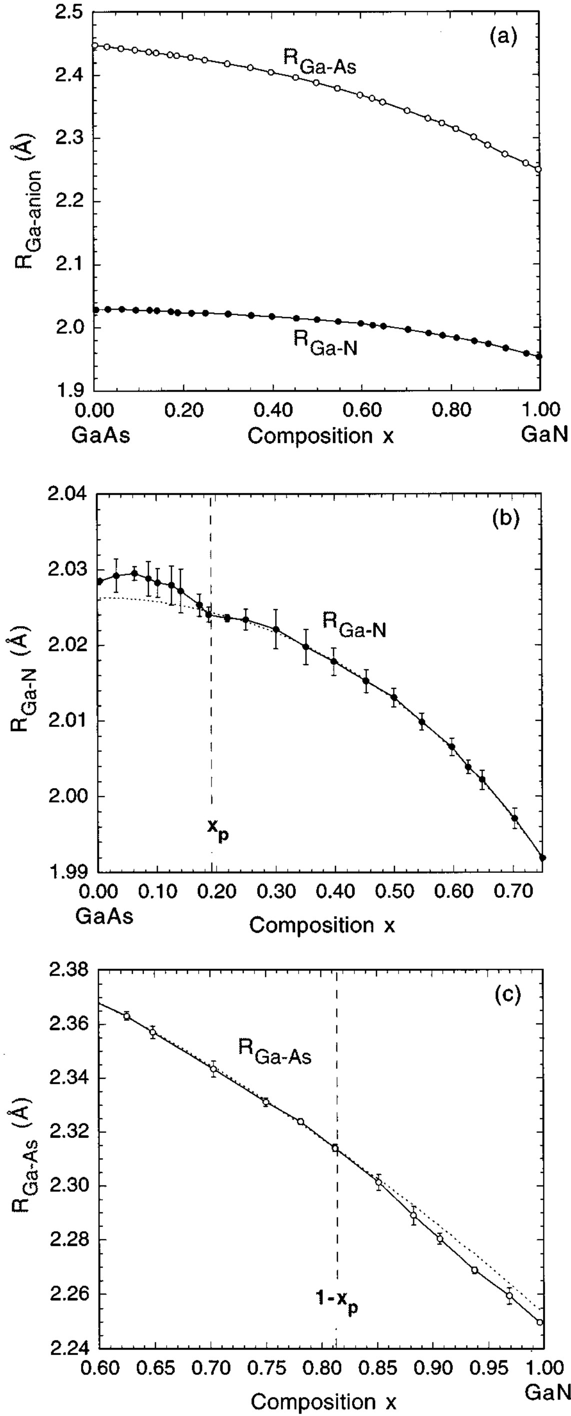

FIG. 1. Variation of the nearest-neighbor bond length $R_{\text{Ga-As}}$ and $R_{\text{Ga-N}}$ in the random $GaAs_{1-x}N_x$ alloys as a function of the nitrogen composition. (b) and (c) show, on an enlarged scale, the behavior of $R_{\text{Ga-N}}$ and $R_{\text{Ga-As}}$ at the critical compositions discussed in the text. The dashed lines correspond to the fourth-order polynomial discussed in the text. The error bars are the statistical fluctuations for different, randomly selected configurations.

loy medium (at $1-x_p \simeq 0.81$) is also accompanied by a small bond length anomaly [see Fig. 1(c)]. In $GaAs_{1-x}P_x$, we find again that the formation of a continuous chain of given bonds leads to an anomaly of these bonds. To quantify these bond length anomalies, we have fitted to a fourth order polynomial the Ga-N, Ga-As, and Ga-P bond lengths for compo-

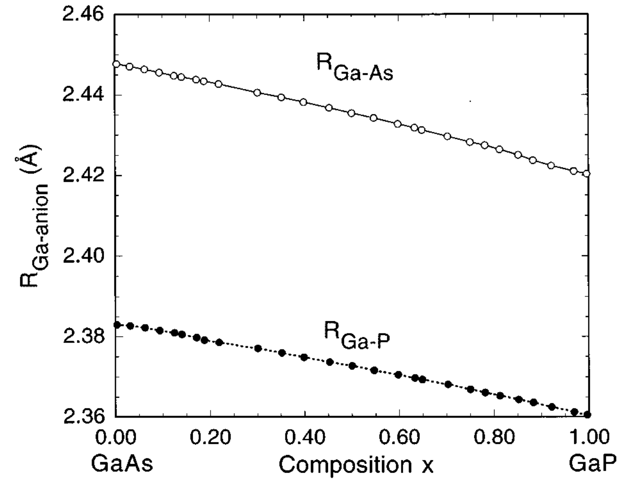

FIG. 2. Variation of the nearest-neighbor bond length $R_{\text{Ga-As}}$ and $R_{\text{Ga-P}}$ in the random $GaAs_{1-x}P_x$ alloys as a function of the P composition. The error bars are the statistical fluctuations for different, randomly selected configurations.

sitions well above the percolation threshold, i.e., in a domain where the bond length $R(x)$ is ''well behaved.'' This polynomial is shown in dashed lines in Figs. 1(b) and 1(c). The fit reproduces our directly calculated values within 99.994%. We then compared the interpolated fit with our actual VFF results close to the percolation threshold [we choose $x=0.06$ for which the statistical VFF error bar is very small; see Figs. 1(b) and 1(c)]. The difference ΔR between the actual and extrapolated bond lengths is shown in Table IX. This indicates that (i) the sign of ΔR is identical to the sign of the difference between the α_{VFF} parameters of the impurity bonds and of the host, and (ii) the bond length anomalies are more pronounced when the absolute difference between the α_{VFF} parameters is larger.

2. *The electronic properties of $GaAs_{1-x}N_x$: Unusual behavior*

We find that the structural percolations evident in Fig. 1 have only a negligible effect on the calculated electronic properties (see the figures below). However, other anomalies are seen in the electronic properties. Figure 3 shows the localization parameters $Q_{\alpha,i}(x)$ of Eq. (3) for the highest occupied (''VBM'') and lowest empty (''CBM'') impurity states for α=Ga, As, and N (compare reference values of pure hosts in Table VI), while Fig. 4 shows the composition variation of the band gap, bowing parameter, and band-edge energies.

TABLE VIII. Comparison of the first-neighbor distances $R_{\text{Ga-As}}$ and $R_{\text{Ga-P}}$ at the impurity limits of the $GaAs_{1-x}P_x$ alloys between our VFF results and EXAFS experiment (Ref. 41). In our calculations, $R^{(o)}_{\text{Ga-As}}$ and $R^{(o)}_{\text{Ga-P}}$, which are the first neighbor distances in the pure GaAs and GaP zinc-blende compounds, have been taken as the experimental values (see Table VII).

Quantity	VFF	Experiment[a]
$R_{\text{Ga-P}}$ (Ga$\underline{\text{As}}$:P)-$R^{(o)}_{\text{Ga-P}}$ (Å)	0.0225	0.021
$R_{\text{Ga-As}}$ (Ga$\underline{\text{P}}$:As)-$R^{(o)}_{\text{Ga-As}}$ (Å)	−0.0275	−0.022

[a]Reference 41.

TABLE IX. The difference ΔR, at $x=0.06$, between the A-C bond length in $AB_{1-x}C_x$ alloys as obtained in actual VFF simulations and the value obtained by fitting $R_{A\text{-}C}(x)$ for the composition domain $x>x_p$, where regular behavior is found. $\Delta\alpha_{\mathrm{VFF}}$ is the difference between the bond-stretching force constants of the impurity and of the host bonds. Note that the value of ΔR is proportional to the value of $\Delta\alpha_{\mathrm{VFF}}$.

Impurity bond	Host	ΔR (Å)	$\Delta\alpha_{\mathrm{VFF}}$ (N/m)
Ga-N	GaAs	+0.003 (0.15%)	+55.11
Ga-As	GaN	−0.006 (−0.26%)	−55.11
Ga-P	GaAs	+0.001 (0.04%)	+6.13
Ga-As	GaP	−0.001 (−0.04%)	−6.13

Analysis of Figs. 3 and 4 suggests three composition regions.

(i) A *nitrogen-impurity region* (for x smaller than 0.1): according to Table VI, nitrogen poses a weak-to-medium perturbation on GaAs. Indeed, at small x in $GaAs_{1-x}N_x$ we find intermediate localization of the CBM wave functions around the N atom [Fig. 3(b)], an increase of the CBM energy [Fig. 4(c)], and of the bowing coefficient [from 6.7 to 7.6 eV, Fig. 4(b)] when x decreases. The band gap in this region decreases rapidly as x increases. This is consistent with the observed rapid redshift of the band-edge photoluminescence with increasing N content in dilute $GaAs_{1-x}N_x$ alloys ($x<0.02$).[45,46]

(ii) *An As-impurity region* for middle and high x (for x higher than 0.4): since As poses a strong perturbation on GaN (viz., Table VI), the effects here are more dramatic than in the nitrogen-impurity region: the arsenic-impurity region is characterized by a very strong localization of VBM wave functions around the As atom [Fig. 3(a)], and a rapid increase of the bowing coefficient [Fig. 4(b)] as x increases. It is also characterized by a rapid decrease of the VBM energy [Fig. 4(c)] and increase of the band gap [Fig. 4(a)] when $x\rightarrow 1$. In this region, the band gap of the *random* alloy can be small (0.4 eV for $x\sim 0.5$), while the band gap of some *ordered* alloys could even be negative [see Fig. 4(a)].

(iii) *An intermediate region* located around x_p, where the alloy properties vary smoothly as a function of composition x: we find that in this region, although still very large (~7 eV) compared to conventional semiconductor alloys, the optical bowing coefficient is nearly composition independent [Fig. 4(b)], and both the CBM and the VBM wave functions are delocalized (Fig. 3).

Our large 512-atom supercell calculation thus confirmed the recent suggestion of Wei and Zunger,[14] based on LDA calculations of smaller cells, that $GaAs_{1-x}N_x$ alloy has one bandlike domain where alloy properties vary smoothly as a function of x (with a composition-independent bowing coefficient) and can be described well by Eq. (1), and two impuritylike domains, where Eq. (1) is not satisfied.

The *basic asymmetry* of $x\rightarrow 0$ (no-gap level for N impurity in GaAs) and $x\rightarrow 1$ (deep level for As impurity in GaN) explains the different behaviors of the physical properties in the N-impurity and As-impurity regions: the N-impurity region shows weak localization of the CBM wave functions around the nitrogen, with an optical bowing coefficient slightly composition dependent, whereas the As-impurity region shows a strong localization of the VBM wave functions around the arsenic, with a bowing coefficient that is very large and strongly dependent on the composition. This asymmetry in the single impurity limits explains also the large compositional range ($\Delta x\simeq 0.6$) of the As-impurity region, compared to the N-impurity region ($\Delta x\simeq 0.1$).

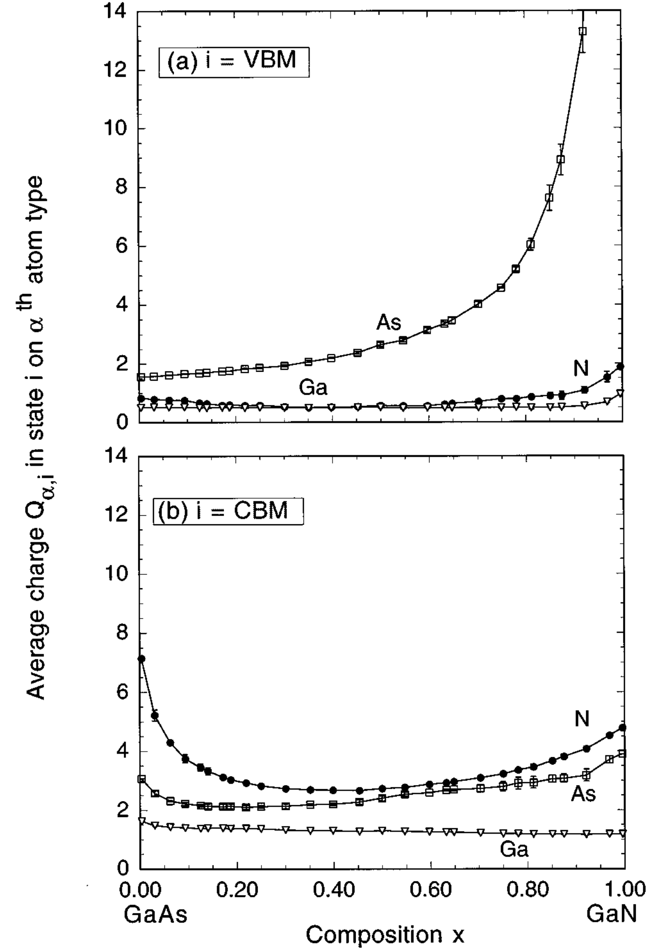

FIG. 3. Variation of the charge localization $Q_{\alpha,i}$ of Eq. (3) for the highest occupied alloy level (i=VBM) and lowest empty alloy level (i=CBM) of atoms α=As,N,Ga of the random $GaAs_{1-x}N_x$ alloys as a function of x. The bars are statistical fluctuations in configurational sampling.

3. The electronic properties of $GaAs_{1-x}P_x$: A "normal" alloy

We now study the alloy properties of the weakly perturbed $GaAs_{1-x}P_x$ system in which no deep levels exist (Table VII). Figure 5 shows, in analogy with Fig. 3, the VBM and CBM localization parameters, while Fig. 6 shows the composition variation of the band gap, bowing parameter and band-edge energies of $GaAs_{1-x}P_x$. The direct to indirect (Γ_c to X_c) crossover occurs in the CBM at $x\simeq 0.50$ [Fig. 6(c)], in good agreement with the experimental results[5–8] of 0.45–0.49, and leads to an abrupt change in the identity of the CBM wave functions [see Fig. 5(b)]. The large fluctuations of Fig. 5(b), for $x\simeq 0.5$, reflect the possibility of the CBM wave functions to have an X_c or Γ_c character at the transition point. We thus report in Fig. 6(b) the optical bowing coefficient for the Γ_{1c} state up to $x=0.4$, and for the X_{1c} state for x higher than 0.6.

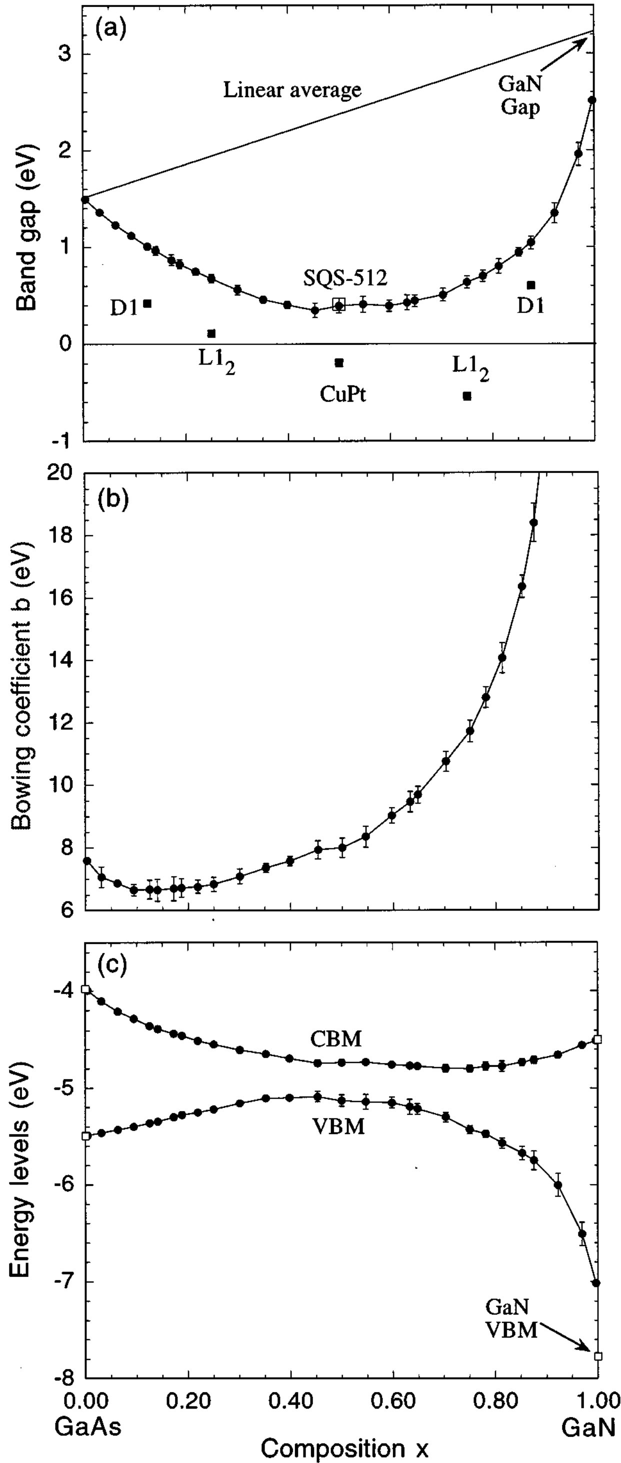

FIG. 4. Variation of electronic energy levels of the random $GaAs_{1-x}N_x$ alloys as a function of x: (a) band gap, (b) bowing coefficient, and (c) VBM and CBM energy levels. The error bars are statistical fluctuations. The symbols in (a) refer to various ordered structures defined in Ref. 20. We have also reported, in Fig. 3(a), the value of the band gap for the 1024-atom supercell of the ''special quasirandom structure'' [called SQS-512 (Ref. 44)]. This structure is selected to simulate very closely random alloys, at $x=0.5$. The band gap for this structure is found to be very close to our configurational averaged results (black dots), suggesting their accuracy.

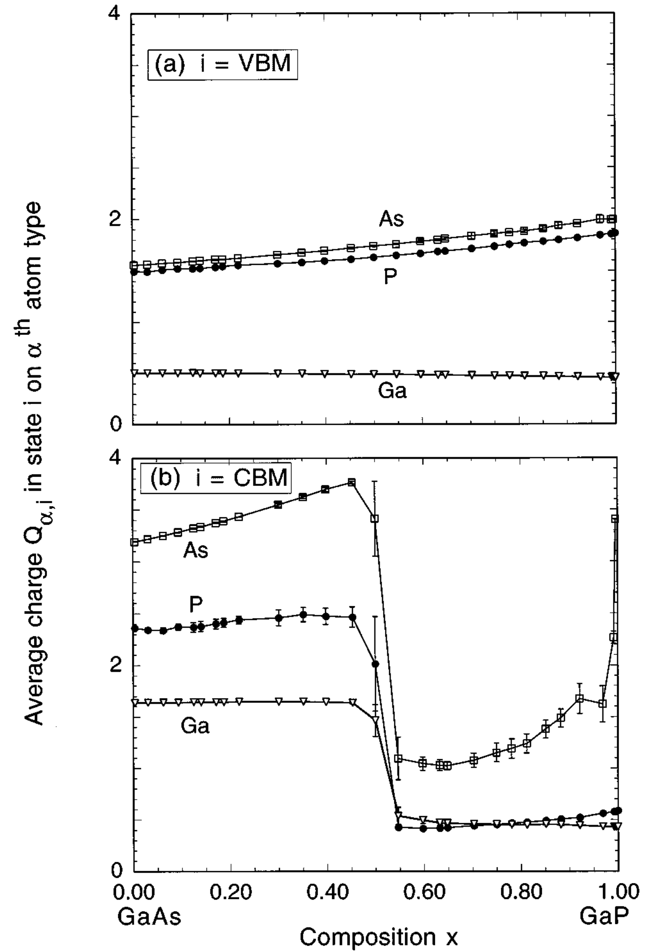

FIG. 5. Variation of the charge localization $Q_{\alpha,i}$ of Eq. (3) for the highest occupied alloy level (i=VBM) and lowest empty alloy level (i=CBM) of atoms α=As,P,Ga of the random $GaAs_{1-x}P_x$ alloys as a function of x. The bars are statistical fluctuations in configurational sampling.

We see that in $GaAs_{1-x}P_x$ the impurity region occurs only in the extreme P-rich alloys (approximately between $x=0.97$ and 1) where the optical X_{1c}-type bowing coefficient ranges from 0.3 to 1 eV and the CBM wave functions are weakly localized around the As impurity atoms. On the other hand, for all other compositions (outside the Γ/X crossover region), this alloy system exhibits normal behavior with spatially extended wave functions, constant and small optical bowing coefficients of about 0.3 eV, in good agreement with experiment[6–8] and LDA-calculated[14,47] results of 0.18–0.28 eV.

IV. DISCUSSION

In studying the $GaAs_{1-x}N_x$ and $GaAs_{1-x}P_x$ alloys, we have found two types of violations of the almost universally expected smooth behavior of the properties of semiconductor alloys with composition. First, the formation of a continuous chain of A-C-A-$C\cdots$ bonds through an $A_xB_{1-x}C$ semiconductor alloy leads to a small anomaly in the A-C bond length at the percolation threshold $x=x_p\simeq0.19-0.20$. These structural anomalies are more pronounced when the difference in

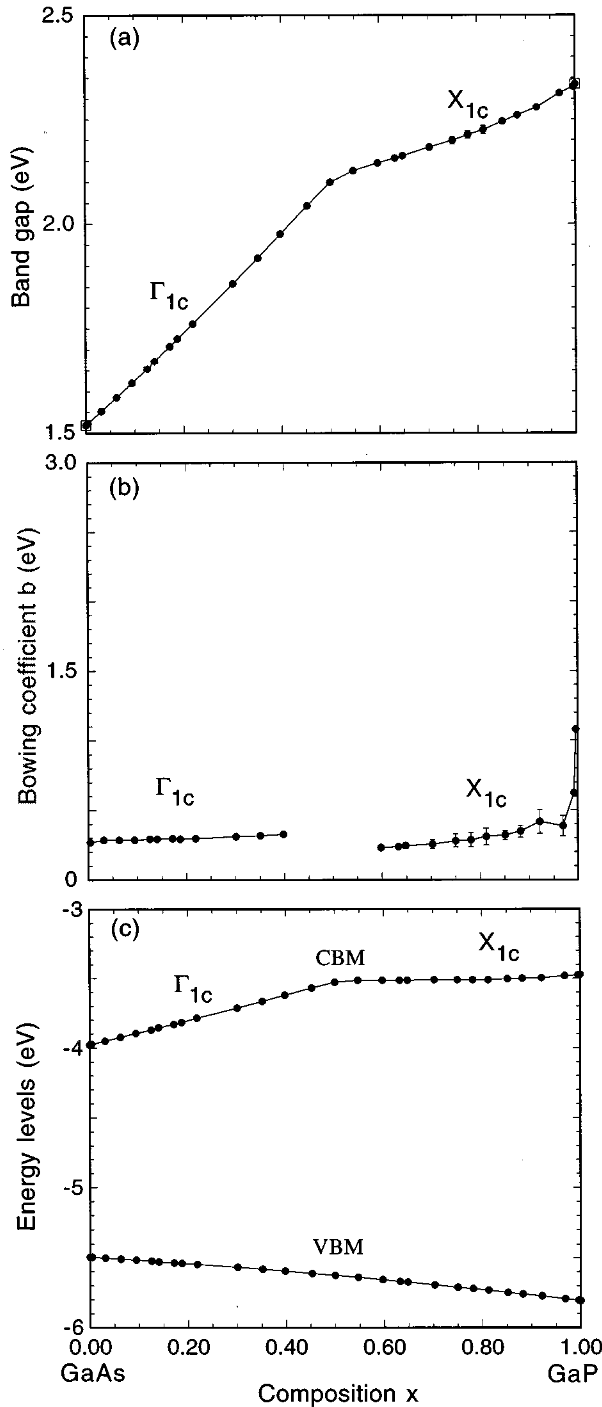

FIG. 6. Variation of electronic energy levels of the random $GaAs_{1-x}P_x$ alloys as a function of x: (a) band gap, (b) bowing coefficient, and (c) VBM and CBM energy levels. The error bars are statistical fluctuations.

stiffness between the A-C and A-B bonds is larger. Second, if the dilute alloys shows a localized deep impurity level in the gap, there will be a composition domain in the concentrated alloy where its electronic properties (e.g., optical bowing coefficient and wave functions) become irregular: the optical bowing coefficient is large and composition-dependent and the wave functions are localized around the impurity atoms. Thus, on a more general note, this study points out that the properties of semiconductor alloys having deep isovalent impurity levels in the dilute alloy limit *may not* be describable by a smooth function of the type of Eq. (1), as previously thought.

In what follows, we will briefly review the literature on *deep isovalent impurities* indicating which alloys are likely to have the anomalies discussed above.

(i) *II-VI alloys*. Optical fluorescence, absorption, surface photo-emf, photoconductivity, and photoluminescence measurements have shown that Cd$\underline{S}$:Te,[48–52] Zn$\underline{S}$:Te,[50,53,54] and Zn$\underline{Te}$:O (Ref. 55) exhibit deep levels inside the band gap of the host, attributed to a single impurity center. The activation energy of these levels has been reported to be 0.22–0.25 eV for Cd$\underline{S}$:Te,[48–51] 0.37–0.40 eV for Zn$\underline{S}$:Te,[50,53,54] and 0.40 eV for Zn$\underline{Te}$:O.[55] In addition, although the *isolated* impurity level of $\underline{CdSe}$:Te and Zn$\underline{Se}$:Te resonated within the host band, cathodoluminescence and photoluminescence experiments have shown that a localized state can nevertheless appear in the host crystal band gap when a few impurity atoms cluster together.[56–60] In that case, the binding energy is somewhat small ($\leqslant$50 meV).[61] We thus expect that the electronic properties of $CdS_{1-x}Te_x$, $ZnS_{1-x}Te_x$, $CdSe_{1-x}Te_x$, and $ZnSe_{1-x}Te_x$ could exhibit a composition domain, where the bowing coefficient is large and composition-dependent and where there is localization of wave functions ($ZnTe_{1-x}O_x$ does not exist as an alloy). A recent experimental study on $ZnS_{1-x}Te_x$ (Ref. 62) corroborates this expectation: the bowing coefficient of this II-VI alloy is large and composition-dependent, ranging from 4.8 eV for $x=0.07$ to 2.5 eV for $x=0.70$. The bowing becomes nearly composition-independent ($b\simeq 2.4$) for higher Te compositions.

(ii) *III-V alloys*. In the same manner, since it has been shown experimentally, both by optical fluorescence and by photoluminescence measurements that Ga$\underline{P}$:Bi,[55] Ga$\underline{P}$:N,[55] and Ga$\underline{N}$:P (Ref. 40) have a deep impurity level (with a binding energy of 0.50,[55] 0.008,[55] and 0.57 eV,[40] respectively), we expect that $GaP_{1-x}Bi_x$ and $GaP_{1-x}N_x$ alloys must also have a composition-dependent bowing coefficient, associated with localization of wave functions.

ACKNOWLEDGMENTS

We wish to thank Y. Zhang for useful discussions, A. Franceschetti for use of some of his codes, W. Lambrecht and B. Segall for communicating the results of Ref. 19, and C. Wolverton for comments on the manuscript. This work is supported by the U.S. Department of Energy, OER-BES-DMS, Grant No. DE-AC36-83-CH10093.

[1] G. Hodes, J. Menassen, and D. Cahen, J. Am. Chem. Soc. **102**, 5964 (1980).
[2] R. T. Delves and B. Levis, J. Phys. Chem. Solids **24**, 549 (1963).
[3] B. Koiller and R. B. Capaz, Phys. Rev. Lett. **74**, 769 (1995).
[4] B. Monemar, K. K. Shih and G. D. Pettit, J. Appl. Phys. **47**, 2604 (1976), and references therein.
[5] M. G. Craford, R. W. Shaw, A. H. Herzog, and W. O. Groves, J. Appl. Phys. **43**, 4075 (1972).
[6] A. Onton and L. M. Foster, J. Appl. Phys. **43**, 5084 (1972).
[7] R. J. Nelson, N. Holonyak, and W. O. Groves, Phys. Rev. B **13**, 5415 (1976).
[8] H. Mathieu, P. Merle, and E. L. Ameziane, Phys. Rev. B **15**, 2048 (1977).
[9] *Physics of Group IV Elements and III-V Compounds*, edited by O. Madelung, M. Schulz, and H. Weiss, Landolt-Bornstein, Numerical Data and Functional Relationships in Science and Technology, Vol. 17, Part a (Springer-Verlag, Berlin, 1982); *GaInAsP Alloy Semiconductors*, edited by T. P. Pearsall (Wiley, New York, 1982); *Physical Properties of III-V Semiconductor Compounds*, edited by S. Adachi (Wiley, New York, 1992).
[10] E. Bruno, B. Ginatempo, E. S. Giuliano, A. V. Ruban, and Yu. Kh. Veliko, Phys. Rep. **249**, 353 (1994).
[11] I. M. Lifshitz, Zh. Eksp. Teor. Fiz. **38**, 1569 (1960) [Sov. Phys. JETP **11**, 1130 (1960)].
[12] E. I. Rogacheva, Jpn. J. Appl. Phys. **32**, 775 (1993).
[13] A. Rubio and M. L. Cohen, Phys. Rev. B **51**, 4343 (1995).
[14] S.-H. Wei and A. Zunger, Phys. Rev. Lett. **76**, 664 (1996).
[15] J. Neugebauer and C. G. Van de Walle, Phys. Rev. B **51**, 10 568 (1995).
[16] J. C. Slater and G. F. Koster, Phys. Rev. **94**, 1498 (1954).
[17] P. N. Keating, Phys. Rev. **145**, 637 (1966).
[18] R. M. Martin, Phys. Rev. B **1**, 4005 (1970).
[19] K. Kim, W. R. L. Lambrecht, and B. Segall, Phys. Rev. B **53**, 16 310 (1996).
[20] Z. W. Lu, S. H. Wei, A. Zunger, S. Frota-Pessoa, and L. G. Ferreira, Phys. Rev. B **44**, 512 (1991).
[21] K. A. Mader and A. Zunger, Phys. Rev. B **50**, 17 393 (1994).
[22] A. Rubio, J. L. Corkhill, M. L. Cohen, E. Shirley, and S. Louie, Phys. Rev. B **48**, 11 810 (1993).
[23] M. Palummo, L. Reining, R. W. Godby, C. M. Bertoni, and N. Bornsen, Europhys. Lett. **26**, 607 (1994).
[24] *Properties of Group-III Nitrides*, edited by J. H. Edgar, Emis Datareviews Series No. 11 (Inspec, London, 1994).
[25] D. S. Kyser and V. Rehn, Phys. Rev. Lett. **40**, 1038 (1978).
[26] R. G. Dandrea and A. Zunger, Appl. Phys. Lett. **57**, 1031 (1990).
[27] D. D. Sell, Phys. Rev. B **6**, 3750 (1972).
[28] R. W. Godby, M. Schlüter, and L. J. Sham, Phys. Rev. B **35**, 4170 (1987).
[29] T. C. Chiang, J. A. Knapp, M. Aono, and D. E. Eastman, Phys. Rev. B **21**, 3513 (1980).
[30] D. E. Aspnes, C. G. Olson, and D. W. Lynch, Phys. Rev. Lett. **37**, 766 (1976).
[31] A. G. Goni, K. Syassen, K. Strossner, and M. Cardona, Semicond. Sci. Technol. **4**, 246 (1989).
[32] S.-H. Wei and A. Zunger, Phys. Rev. B **39**, 3279 (1989).
[33] K. Reinmann, M. Holtz, K. Syassen, Y. C. Lu, and E. Bauser, Phys. Rev. B **44**, 2985 (1991).
[34] D. Olego, M. Cardona, and H. Müller, Phys. Rev. B **22**, 894 (1980).
[35] A. Azema, J. Botineau, F. Gires, and A. Saissy, J. Appl. Phys. **49**, 24 (1987).
[36] J. M. Chamberlain, P. E. Simmonds, R. A. Stradling, and G. G. Bradley, in *Proceedings of the 11th International Conference on the Physics of Semiconductors, Warsaw, 1972*, edited by M. Miasek (PWN–Polish Scientific, Warsaw, 1972), p. 1016.
[37] L.-W. Wang and A. Zunger, J. Chem. Phys. **100**, 2394 (1994).
[38] We find in GaAs:N a N-pertrubed CBM whose energy depends on the impurity concentration: for $x=0.001$, 0.002, and 0.004 (one nitrogen impurity in a 1728-, 1000-, and 512-atom supercell), the difference between the band gap of pure GaAs and the alloys band gap is 6, 11, and 23 meV, respectively. In addition, we find an impurity level, strongly localized around the nitrogen, located 250 meV *above* the GaAs CBM. This is the nitrogen impurity state which drops into the GaAs band gap when applying pressure (Ref. 39).
[39] X. Liu, M.-E. Pistol, and L. Samuelson, Phys. Rev. B **42**, 7504 (1990).
[40] J. I. Pankove and J. A. Hutchby, J. Appl. Phys. **47**, 5387 (1976).
[41] J. B. Boyce and J. C. Mikkelsen, in *Ternary and Multiternary Compounds*, edited by S. Deb and A. Zunger (Materials Research Society, Pittsburgh, 1987), p. 359.
[42] B. I. Shklovskii and A. L. Efros, *Electronic Properties of Doped Semiconductors* (Springer-Verlag, Heidelberg, 1984).
[43] D. Stauffer and A. Aharony, *Introduction to Percolation Theory* (Taylor and Francis, London, 1992).
[44] K. A. Mader and A. Zunger, Phys. Rev. B **51**, 10 462 (1995).
[45] M. Weyers, M. Sato, and H. Ando, Jpn. J. Appl. Phys. **31**, L853 (1992).
[46] M. Kondow, K. Uomi, K. Hosomi, and T. Mozume, Jpn. J. Appl. Phys. **33**, L1056 (1994).
[47] R. Magri, S. Froyen, and A. Zunger, Phys. Rev. B **44**, 7947 (1991).
[48] J. D. Cuthbert and D. G. Thomas, J. Appl. Phys. **39**, 1573 (1968).
[49] D. M. Roessler, J. Appl. Phys. **41**, 4589 (1970).
[50] D. Hennig, O. Goede, and W. Heimbrodt, Phys. Status Solidi B **113**, K163 (1982).
[51] O. Goede and W. Heimbrodt, Phys. Status Solidi B **110**, 175 (1982).
[52] O. F. Vyvenko, I. A. Davydov, V. G. Luchina, and S. L. Tselishchev, Fiz. Tekh. Poluprovodn. **25**, 1745 (1991) [Sov. Phys. Semicond. **25**, 1050 (1991)].
[53] G. W. Iseler and A. J. Strauss, J. Lumin. **3**, 1 (1970).
[54] T. Fukushima and S. Shionoya, Jpn. J. Appl. Phys. **12**, 549 (1973).
[55] J. D. Cuthbert and D. G. Thomas, Phys. Rev. **154**, 763 (1967).
[56] A. Reznitsky, S. Permogorov, S. Verbin, A. Naumov, Yu. Korostelin, V. Novozhilov, and S. Prokov'ev, Solid State Commun. **52**, 13 (1984).
[57] H. Stolz, W. Von Der Osten, S. Permogorov, A. Reznitsky, and A. Naumov, J. Phys. C **21**, 5139 (1988).
[58] S. Permogorov, A. Reznitsky, A. Naumov, H. Stolz, and W. Von Der Osten, J. Phys. C **1**, 5125 (1989).
[59] I. V. Akimova, A. M. Akhekyan, V. I. Kozlovskii, Yu. Korostelin, and P. V. Shapkin, Fiz. Tverd. Tela (Leningrad) **27**, 1734 (1985) [Sov. Phys. Solid State **27**, 1041 (1985)].
[60] O. Goede and D. Hennig, Phys. Status Solidi B **119**, 261 (1983).
[61] R. Baltrameyunas, V. Gavryushin, G. Rachyukaitis, V. Ryzhikov, A. Kazlauskas, and V. Kubertavichyus, Fiz. Tekh. Poluprovodn. **22**, 1163 (1988) [Sov. Phys. Semicond. **22**, 738 (1988)].
[62] I. K. Sou, K. S. Wong, Z. Y. Yang, H. Wang, and G. K. L. Wong, Appl. Phys. Lett. **66**, 1915 (1995).